Luminescent Properties of CdS Nanoclusters Dispersed in Solution –Effects of size and surface termination

Masayuki Okamura[a], Kojiro Ebina[a], Seiji Akimoto[b], Iwao Yamazaki[b], and Kohei Uosaki[a]*,

[a]Physical Chemistry Laboratory, Division of Chemistry, Graduate School of Science, Hokkaido University, Sapporo 060-0810, Japan.

[b]Department of Molecular Chemistry, Graduate School of Engineering, Hokkaido University, Sapporo 060-8628, Japan.

*To whom correspondence should be addressed. TEL: +81-11-70-3812 FAX: +81-11-706-3440 E-mail: uosaki@pcl.sci.hokudai.ac.jp

Abstract

Steady state and ultrafast transient luminescent properties of CdS nanoclusters prepared by the AOT/n-heptane reverse micelle method and those modified with 2-mercaptoethanesulfonate were investigated in heptane and water, respectively. A very short luminescence component (~ 200 fs) was observed for the first time for CdS nanoclusters dispersed in solution. The luminescence mechanism of CdS nanoclusters is proposed.

1. Introduction

Metal and semiconductor nanoclusters have recently attracted much interest because of their unique optical and electronic properties, which are different from those of bulk materials [1-12]. Semiconductor nanoclusters, the radii of which are smaller than the bulk exciton Bohr radius, constitute a class of materials of intermediate nature between molecular and bulk forms of matter. Quantum confinement of both electrons and holes in all three dimensions leads to an increase in the effective band gap of the material with decreasing cluster size. Consequently, both optical absorption and emission of nanoclusters shift to blue (higher energy) with decrease in sizes of the clusters [13]. There are numerous reports on dynamics of electron-hole recombination using ultrafast transient absorption spectroscopy [14-18].

II-VI semiconductor nanoclusters are known to be photoluminescence materials and are used for nonlinear optics and laser applications [14]. Although many studies on luminescent properties of II-VI semiconductor nanoclusters have been published in the last two decades [13, 19-26], the luminescence mechanism in nanoclusters has not been fully elucidated. Based on results of detailed investigations of the excitonic emission by various groups, it is considered that at least one of the charge carriers involved in the recombination process is trapped in very shallow traps [20, 27, 28]. O'Neil et al. [20] and Eychmuller et al. [27] suggested that the electrons are first trapped and then recombine with free holes after thermally returning to the conduction band. On the other hand, Bawendi et al. [28] postulated that there is a strong resonance between free holes and holes in shallow traps. The luminescence, which is strongly red shifted from the absorption, is usually assigned to the recombination of trapped holes.

Optical and luminescent properties of semiconductor nanoclusters are very sensitive to the surface chemical structure and the environment around nanoclusters [29]. Chemical modification of the surface of semiconductor nanoclusters by capping with organic reagents seems to be one of the most effective methods to control these properties. It is therefore very important to clarify the effect of the capping agent on various properties of semiconductor nanoclusters [30].

In this study, we investigated the steady state and ultra-fast transient luminescent properties of CdS nanocluster prepared by the Aerosol-OT (AOT)/n-heptane reverse micelle method (AOT-CdS nanoclusters) as well as those of CdS nanoclusters modified with 2-mercaptoethanesulfonate (SO_3-CdS nanoclusters), which can be used as a building block for the construction of mono- and multilayers on a substrate using a cationic polymer or other cationic groups [31]. A model for luminescence from CdS nanoclusters and the cause of the change in luminescence characteristics by surface modification are proposed.

2. Experimental

2.1 Materials

Ethanol (superpure grade), pyridine (superpure grade), diethyl ether (superpure grade), 1-butanol (superpure grade), acetone (superpure grade), bis(2-ethylhexyl) sodium sulfosuccinate (AOT, pure grade) and $Na_2S{\cdot}9H_2O$ were purchased from Wako Pure Chemicals, and $Cd(ClO_4)_2{\cdot}6H_2O$ was obtained from Kishida Chemicals. 2-Mercaptoethanesulfonate (97%) was obtained from Aldrich, and toluene (spectroscopy grade), n-heptane (spectroscopy grade) and methanol (spectroscopy grade) were purchased from Dojindo Laboratory. All chemicals were used without

further purification. Ultrapure water was obtained using a Milli-Q water purification system (Millipore). Ar(99.999%) and N_2 (99.99%) were obtained from Air Water.

2.2 Preparation of CdS nanoclusters

CdS nanoclusters were prepared in AOT/heptane reversed micelles [9, 32-35]. Typically, 100 ml n-heptane solution of 0.2 M AOT was prepared in two separate Schlenck tubes. An aqueous solution of $Cd(ClO_4)_2 \cdot 6H_2O$ (0.4 M) was added to one solution, while an aqueous solution of $Na_2S \cdot 9H_2O$ (0.3 M) was added to the other solution with a molar ratio of $W = [H_2O]/[AOT]$ for both solutions [36]. After each solution had been stirred individually for 1-2 h, they were mixed together and stirred for another 1 h, resulting in the formation of CdS nanoparticles in the reversed micelles.

Surface-modified CdS nanoparticles were prepared by the method reported by Miyake et al. [37]. Aqueous solution of 0.3 M 2-mercaptoethanesulfonate was added to 100 ml of the reversed micelles solution containing CdS nanoparticles and stirred for 2 h, resulting in the formation of CdS nanoparticles covered with 2-mercaptoethanethiol. The thiol-covered CdS nanoparticles were obtained as precipitate after being dried under vacuum. The nanoparticles were sequentially washed with pyridine, n-heptane, diethyl ether, 1-butanol, acetone, and methanol.

2.3 UV-visible spectroscopy, fluorescence spectroscopy and luminescence lifetime measurement

UV-visible spectra of CdS nanoparticles in solution were obtained using a Hitachi U-3300 spectrometer. Steady-state luminescence measurements were carried out using a Hitachi F-2000 spectrometer.

Ultrafast luminescence lifetime measurements were carried out by using a femto second luminescence up-conversion system, the details of which have been given elsewhere [38]. Briefly, the second harmonic of a Ti:Sapphire laser (Spectra-Physics, Tsunami, 840 nm, 80 MHz) pumped with a diode-pumped solid state laser (Spectra-Physics, Millennia X) was used as an excitation source. The fundamental pulses are split into two beams; one is frequency-doubled by a BBO crystal (420 nm) to excite the sample, and the other beam serves as a gate pulse. The gate pulse traverses a variable optical delay of 2 μm/step (6.7 fs), while the excitation pulse traverses a fixed delay before being focused into a 1 mm sample cell. The fluorescence emission and the gate pulse are focused into a 0.5 mm thick BBO crystal in a type-1 phase matching geometry. To avoid polarization effects, the angle between the polarizations of the excitation and probe beams were set to the magic angle by a λ/2 plate. The sum-frequency signal of the Raman line in pure benzene excited with the second harmonic yielded an instrumental response function of 200 fs FWHM. All measurements were carried out at room temperature.

3. Results

3.1 Luminescent properties of AOT-CdS nanoclusters

Figures 1 (A) and (B) show absorption spectra and steady state luminescent spectra excited at 380 nm, respectively, of AOT-CdS nanoclusters with various AOT/n-heptane ratios (W = (a) 1, (b) 3, (c) 4.5, (d) 6, and (e) 8). As W decreased, the absorption edge as well as excitation peaks were shifted to a shorter wavelength, although an exciton peak was not clearly observed in the case of W = 8. These results are in good agreement with the previously reported results [9, 33, 34, 39]. The sizes of

AOT-CdS nanoclusters for W = 1, 3, 4.5, 6, and 8 were estimated to be 1.1 nm, 1.4 nm, 2.2 nm, 2.8 nm and 4.3 nm, respectively [13, 40]. The absorption edge reflects the energy gap of a CdS nanocluster, which increased with decrease in size due to the quantum size effect. The exciton peak was not as sharp as expected, possibly because of the wide size distribution.

Luminescence peaks were very broad and peak wavelength was much larger than the absorption edge. These results suggest that the luminescence was not due to direct band-to-band recombination but was surface trap luminescence. Luminescence due to the recombination of electrons and holes both in the surface traps has been reported by Harruff et al. [13]. They suggested that shallow trap luminescence and exciton luminescence also contribute to the broad luminescence. As the size of the CdS nanocluster increases, energy differences between electrons and hole traps decrease, leading to the red shift of the luminescence [13].

Figure 2 shows luminescence decay curves in the ps time domain of the AOT-CdS nanoclusters (W = 4.5) in heptane monitored at (a) 530 nm, (b) 580 nm, and (c) 630 nm. This is the first report of ultrafast luminescence decay behavior of CdS nanoclusters dispersed in solution, although ultrafast transient luminescence of CdS nanocluster doped glass has been measured by the femtosecond up-conversion method [41, 42]. Luminescence decay curves monitored at 530 and 580 nm can be fitted by a sum of three exponential decay curves with time constants of 200 fs, 1.9 ps and > 1 ns and the decay monitored at 630 nm can be fitted with two exponential curves with time constants of 1.9 ps and > 1 ns. These results suggest that at least three kinds of emission processes existed in the CdS nanocluster. Luminescence lifetimes are summarized in Table 1(a). The luminescence lifetime of each process did not depend on the probe

wavelengths but the contribution of the long lifetime component was smaller as the probe wavelength became shorter. The long lifetime component has been suggested to be due to recombination of electrons and holes trapped at the surface states [13, 19].

Figure 3 shows femtosecond luminescence decay curves of the AOT-CdS nanoclusters (W = 8) observed at (a) 600 nm, (b) 650 nm, and (c) 700 nm in heptane. The decay behaviors are essentially the same as those observed for the CdS nanoclusters of W = 4.5. Luminescence decay curves monitored at 600 nm can be fitted by a sum of three exponential decay curves with time constants of 550 fs, 3.4 ps and > 1 ns, and the decay monitored at 650 nm can be fitted with two exponential decay curves with time constants of 3.7 ps and > 1 ns. At 700 nm, only a long lifetime component was observed. Luminescence lifetimes are summarized in Table 1(b).

3.2 Luminescent properties of SO_3-CdS nanoclusters

Figure 4 shows (A) absorption spectra and (B) luminescence spectra of SO_3-CdS nanoclusters (W = 8) dispersed in water. The absorption spectrum of an SO_3-CdS nanocluster was almost the same as that of an AOT-CdS nanocluster, showing that the size of CdS nanocluster did not change after the surface modification. Figure 4(B) clearly shows luminescence was quenched but the luminescence peak did not shift after the surface modification. Similar result was reported by Herron et al. [43]. They suggested that the thiolate-capping agents was responsible for the reduction of the luminescence intensity by removing the sulfur anion vacancies [43]. These results indicate that the number of surface states originally present decreased and no new surface states were produced.

Figure 5 shows femtosecond luminescence decay curves of SO_3-CdS

nanoclusters (W=8) monitored at (a) 600 nm, (b) 650 nm and (c) 700 nm in aqueous solution. Luminescence lifetime decay curves monitored at 600 nm can be fitted by a sum of three exponential decay curves with time constants of 220 fs, 2.6 ps and > 1 ns, and the decay monitored at 650 nm can be fitted with two exponential decay curves with time constants of 2.6 ps and > 1 ns. At 700 nm, only a long lifetime component was observed. Lifetimes are summarized in Table 1 (c). Although the lifetime of each decay component was the same as that of the AOT-CdS nanoclusters (W = 8), the contribution of the shorter lifetime component is much greater in the case of SO_3-CdS nanoclusters.

4. Discussion

Very fast rise (< 100 fs) of luminescence suggests that electrons and holes are either created directly at the surface trap site since the wave function extends to the surface region for such quantum-mechanically confined nanoclusters or generated inside the nanoclusters and then migrate to the surface trap site within 100 fs [15].

Although three decay components with lifetimes of several hundreds of fs, several ps and > 1 ns were observed in the case of AOT-CdS nanoclusters (W = 4.5 and 8), a very fast luminescence decay component (200 fs for W = 4.5 or 550 fs for W = 8) was observed only when the luminescence was monitored at relatively short wavelengths. This suggests that the very fast component is due to band-to-band recombination. Since the energy gaps of AOT-CdS (W=4.5) and AOT-CdS (W=8) were 2.88 eV (430 nm) and 2.47 eV (500 nm), respectively, the probe wavelengths corresponded only to the foot of the luminescence peak. Steady state band edge luminescence was not observed because electrons in the valence band and holes in the

conduction band moved to the traps very quickly, i.e., within 200 - 500 fs.

Lifetimes of 1.9 - 3.7 ps were in good agreement with those for CdS doped glass determined by visible pump - IR absorption and luminescence lifetime measurements [41, 42]. It has been suggested that this component is related to shallow traps. Thus, we can conclude that the luminescence component with lifetimes of 1.9 - 3.7 ps observed in the present study was from shallow traps.

Luminescence of much longer lifetime should be surface trap luminescence, which is the dominant component in the steady state luminescence. Since the energy of this luminescence is smaller than that of the band-to-band luminescence and that of the shallow trap luminescence, the component of very long life became dominant when the luminescence decay was monitored at relatively long wavelength.

In the case of the SO_3-CdS nanoclusters, the steady state luminescence intensity decreased and the contribution of luminescence of very long lifetime decreased, although the lifetime of each component was essentially the same as that of the AOT-CdS nanoclusters. This may be explained by considering that the luminescence from the surface trap was quenched by the surface modification by thiolate but the detailed understanding of the mechanism requires information of lifetimes of excited electrons and holes.

5. Conclusion

Steady state and ultrafast transient luminescent properties of CdS nanoclusters prepared by AOT/n-heptane reverse micelle method and those modified with 2-mercaptoethanesulfonate were investigated in heptane and water, respectively. A very short luminescence component (~ 200 fs) was observed for the first time for CdS

nanoclusters dispersed in solution. The following three luminescence channels are proposed: 1. band-to-band luminescence with a decay constant of 100-550 fs, 2. luminescence from the shallow traps with a decay constant of 1.9 – 3.7 ps, and 3. luminescence from surface traps with a very long decay constant. The last component dominated in the steady state luminescence and was decreased by surface modification by thiolate.

To clarify the carrier dynamics of CdS nanoclusters in more detail, it is essential to probe the lifetimes of free carriers, i.e., electrons and holes, independently by IR transient measurements, which we are currently carrying out using a femtosecond visible pump - IR probe system.

Acknowledgements

We are grateful to Dr. T. Torimoto for instruction in the preparation of the thiol covered CdS nanoclusters. This work is partially supported by a Grant-in-Aid for Scientific Research (KAKENHI) in Priority Area of “Molecular Nano Dynamics” (No. 16072202) from Ministry of Education, Culture, Sports, Science and Technology.

References

[1] D. Routkevitch, A. A. Tager, J. Haruyama, D. Almawlawi, M. Moskovits, and J. M. Xu, *IEEE Trans. Electron Dev.,* **43**, 1646 (1996).

[2] V. Erokhin, P. Facci, S. Carrara, and C. Nicolini, *Biosens. Bioelectron.,* **12**, 601 (1997).

[3] R. Verberk, A. M. van Oijen, and M. Orrit, *Phys. Rev. B,* **6623**, 3202 (2002).

[4] H. Weller, U. Koch, M. Gutierrez, and A. Henglein, *Ber. Bunsen-Ges.,* **88**, 649 (1984).

[5] L. Sheeney-Haj-Ichia, J. Wasserman, and I. Willner, *Adv. Mater.,* **14**, 1323 (2002).

[6] S. G. Hickey, D. J. Riley, and E. J. Tull, *J. Phys. Chem. B,* **104**, 7623 (2000).

[7] H. Yonemura, M. Yoshida, S. Miyake, and S. Yamada, *Electrochem.,* **67**, 1209 (1999).

[8] T. Nakanishi, B. Ohtani, and K. Uosaki, *Jpn. J. Appl. Phys.,* **38**, 518 (1999).

[9] T. Nakanishi, B. Ohtani, and K. Uosaki, *J. Phys. Chem. B,* **102**, 1571 (1998).

[10] T. Nakanishi, B. Ohtani, and K. Uosaki, *J. Electroanal. Chem.,* **455**, 229 (1998).

[11] J. Nanda, K. S. Narayan, B. A. Kuruvilla, G. L. Murthy, and D. D. Sarma, *Appl. Phys. Lett.,* **72**, 1335 (1998).

[12] T. Torimoto, N. Tsumura, H. Nakamura, S. Kuwabata, T. Sakata, H. Mori, and H. Yoneyama, *Electrochim. Acta,* **45**, 3269 (2000).

[13] B. A. Harruff and C. E. Bunker, *Langmuir* **19**, 893 (2003).

[14] V. I. Klimov and D. W. Mcbranch, *Phys. Rev. B,* **55**, 13173 (1997).

[15] V. I. Klimov and D. W. Mcbranch, *Phys. Rev. Lett.,* **80**, 4028 (1998).

[16] V. I. Klimov, *J. Phys. Chem. B,* **104**, 6112 (2000).

[17] V. I. Klimov and M. G. Bawendi, *MRS Bulletin,* **26**, 998 (2001).

[18] U. Banin, G. Cerullo, A. A. Guzelian, A. P. Alivisatos, and C. V. Shank, *Phys. Rev. B,* **55**, 7059 (1997).

[19] N. Chestnoy, T. D. Harris, R. Hull, and L. E. Brus, *J. Phys. Chem.,* **90**, 3393 (1986).

[20] M. O'Neil, J. Marohn, and G. McLendon, *J. Phys. Chem.,* **94**, 4356 (1990).

[21] J. H. Hodak, A. Henglein, and G. V. Hartland, *J. Phys. Chem. B,* **104**, 9954 (2000).

[22] M. Braun, S. Link, C. Burda, and M. El-Sayed, *Chem. Phys. Lett.,* **361**, 446 (2002).

[23] P. V. Kamat, *Chem. Rev.,* **93**, 267 (1993).

[24] A. Henglein, *Chem. Rev.,* **89**, 1861 (1989).

[25] A. P. Alivisatos, *J. Phys. Chem.,* **100**, 13226 (1996).

[26] A. L. Efros, D. J. Lockwood, L. Tsybeskov (Eds.), *Semiconductor Nanocrystals: From Basic Principles to Applications*, Kluwer/Plenum, New York, 2003.

[27] A. Eychmuller, A. Hasselbarth, L. Katsikas, and H. Weller, *Ber. Bunsenges. Phys. Chem.* **95**, 79 (1991).

[28] M. G. Bawendi, P. J. Carroll, W. L. Wilson, and L. E. Brus, *J. Chem. Phys.,* **96**, 946 (1992).

[29] M. L. Steigerwald and L. E. Brus, *Acc. Chem. Res.,* **23**, 183 (1990).

[30] T. Torimoto, H. Uchida, T. Sakata, H. Mori, and H. Yoneyama, *J. Am. Chem. Soc.,* **115**, 1874 (1993).

[31] K. Uosaki, M. Okamura, and K. Ebina, *Faraday Discuss.,* **125**, 39 (2004).

[32] M. L. Steigerwald, A. P. Alivisatos, J. M. Gibson, T. D. Harris, R. Kortan, A. J.

Muller, A. M. Thayer, T. M. Duncan, D. C. Douglass, and L. E. Brus, *J. Am. Chem. Soc.,* **110**, 3046 (1988).

[33] T. Nakanishi, B. Ohtani, and K. Uosaki, *Jpn. J. Appl. Phys.,* **36**, 4053 (1997).

[34] T. Nakanishi, B. Ohtani, K. Shimazu, and K. Uosaki, *Chem. Phys. Lett.,* **278**, 233 (1997).

[35] A. R. Kortan, R. Hull, R. L. Opila, M. G. Bawendi, M. L. Steigerwald, P. J. Carroll, and L. E. Brus, *J. Am. Chem. Soc.,* **112**, 1327 (1990).

[36] J. G. Gordon II and J. D. Swalen, *Opt. Commun.,* **22**, 374 (1977).

[37] M. Miyake, H. Matsumoto, M. Nishizawa, T. Sakata, H. Mori, S. Kuwabata, and H. Yoneyama, *Langmuir* **13**, 742 (1997).

[38] S. Akimoto, T. Yamazaki, I. Yamazaki, and A. Osuka, *Chem. Phys. Lett.,* **309**, 177 (1999).

[39] B. H. Robinson, T. F. Towey, S. Zourab, A. J. W. G. Visser, and A. v. Hoek, *Colloid. Surf.,* **61**, 175 (1991).

[40] P. E. Lippens and M. Lannoo, *Phys. Rev. B,* **39**, 10935 (1989).

[41] V. Klimov, P. Haring Bolivar, and H. Kurz, Phys. Rev. B, 53, 1463 (1996).

[42] V. I. Klimov, C. J. Schwarz, D. W. McBranch, C. A. Leatherdale, and M. G. Bawendi, *Phys. Rev. B,* **60**, R2177 (1999).

[43] N. Herron, Y. Wang, and H. Eckert, *J. Am. Chem. Soc.,* **112**, 1322 (1990).

Figure captions

Figure 1. (A) Absorption and (B) luminescence spectra of AOT-CdS nanoclusters of various sizes. (a) W=1, (b) W=3, (c) W=4.5, (d) W=6, and (e) W=8. Luminescence spectra were obtained at 350 nm excitation.

Figure 2. Femtosecond luminescence decay curves of AOT-CdS nanoclusters (W = 4.5) with 400 nm excitation probed at (a) 530 nm, (b) 580 nm, and (c) 630 nm)

Figure 3. Femtosecond luminescence decay curves of AOT-CdS nanoclusters (W = 8) monitored at (a) 600 nm, (b) 650 nm and (c) 700 nm. All samples were excited at 400 nm.

Figure 4. (A)Absorption and (B) luminescence spectra of AOT-CdS nanoclusters (W=8) (dotted line) and SO_3-CdS nanocluster (W=8) (solid line). All samples were excited at 400 nm for the luminescence measurement.

Figure 5. Femtosecond luminescence decay curves of SO_3-CdS nanoclusters (W = 8) monitored at (a) 600 nm, (b) 650 nm and (c) 700 nm. All samples were excited at 400 nm.

Figure 2

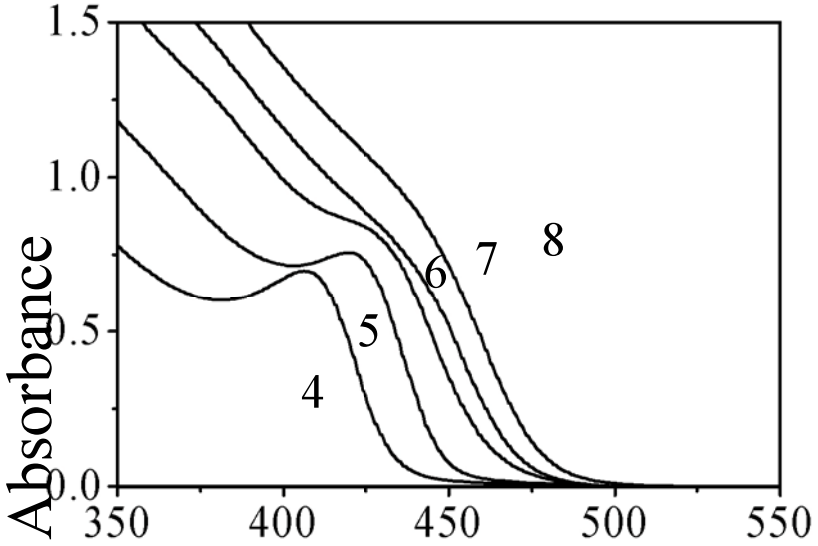

Wavelength / nm

Figure 3

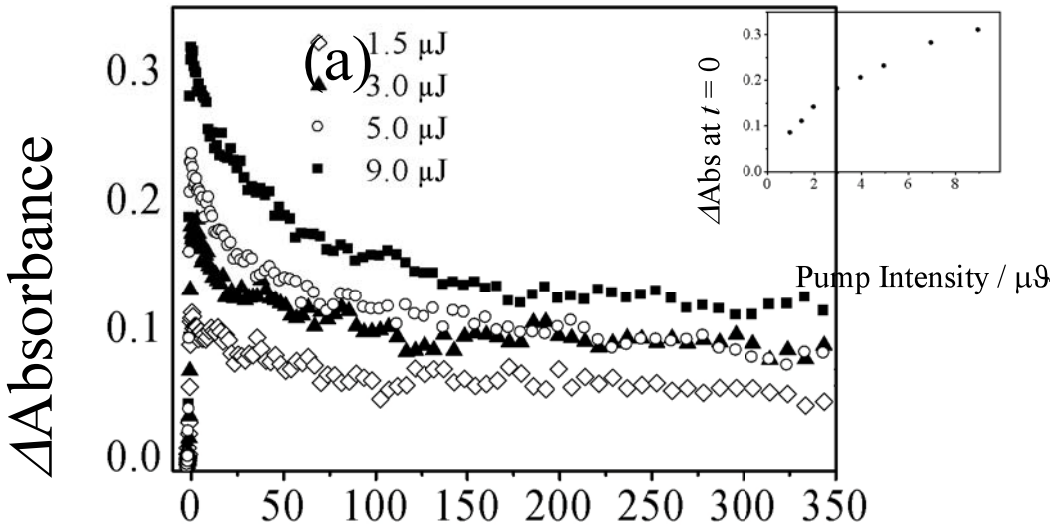

Time / ps

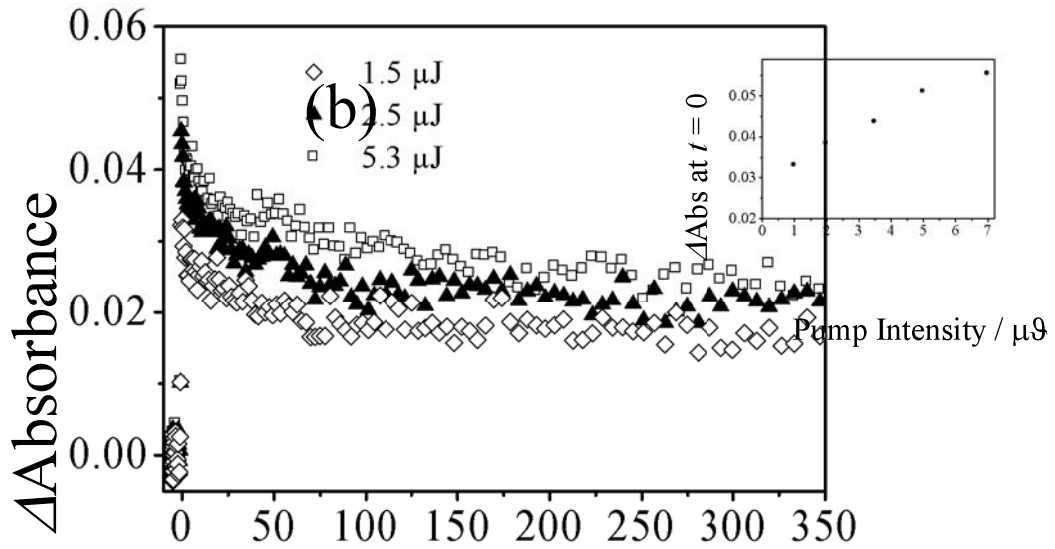

Time / ps

Figure 4

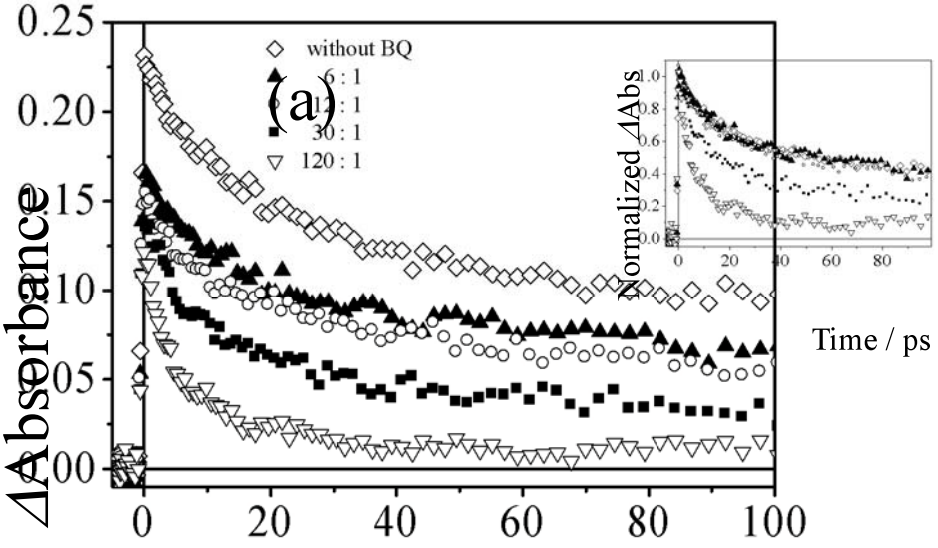

Time / ps

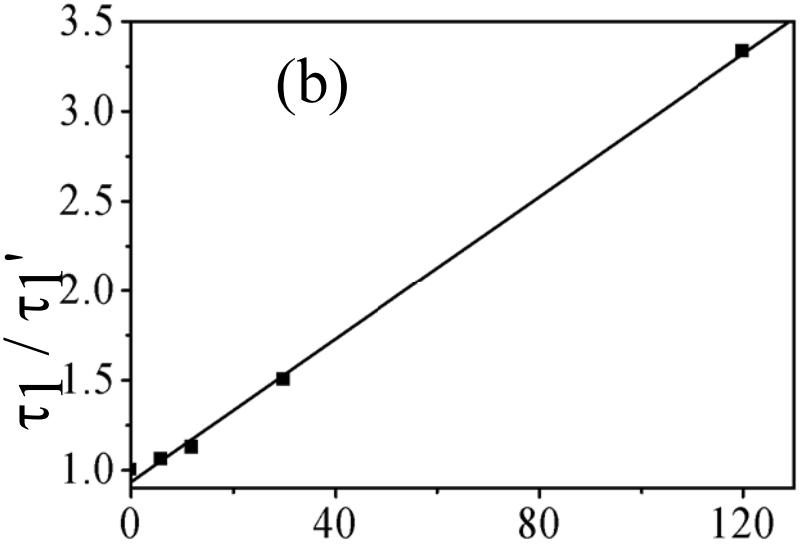

$[MV^{2+}]$ / [CdS]

Figure 5

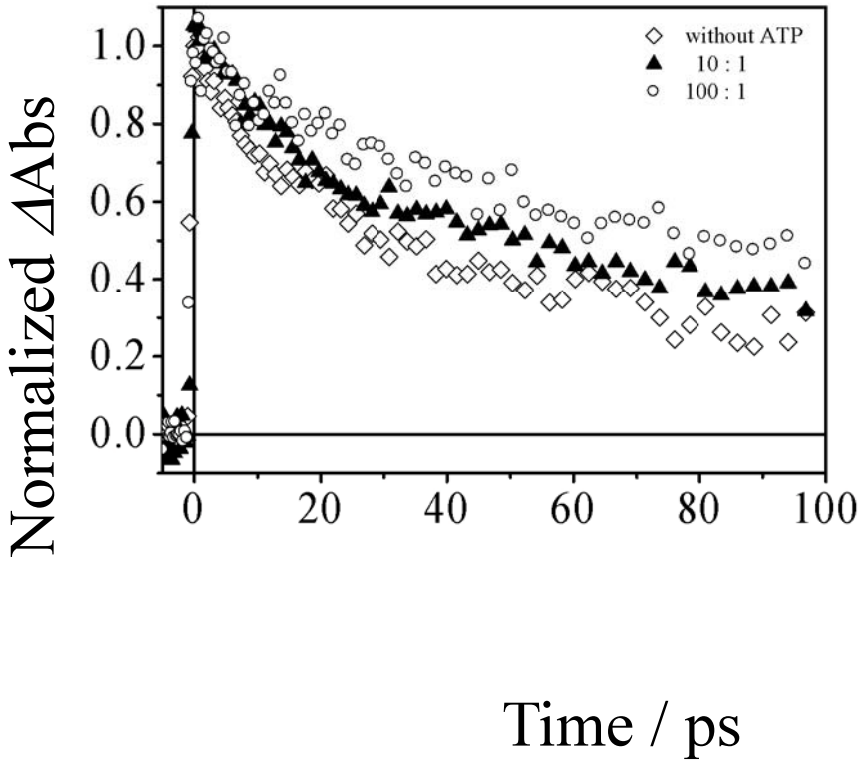
Normalized ΔAbs
1.0
0.8
0.6
0.4
0.2
0.0
0
20
40
60
80
100
without ATP
10 : 1
100 : 1
Time / ps

Figure 6

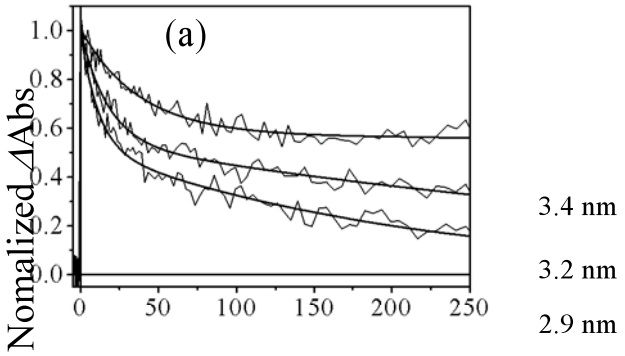

Time / ps

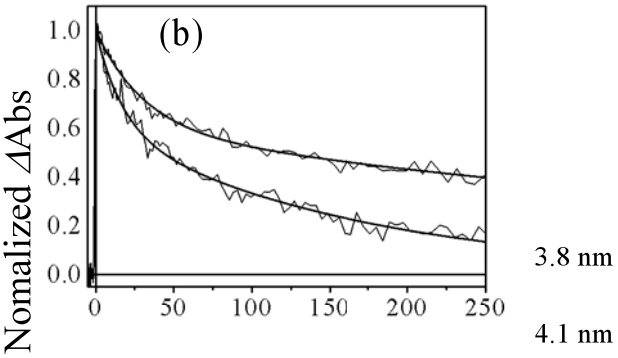

Time / ps

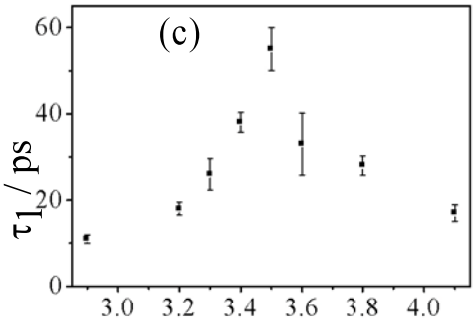

Diameter / nm

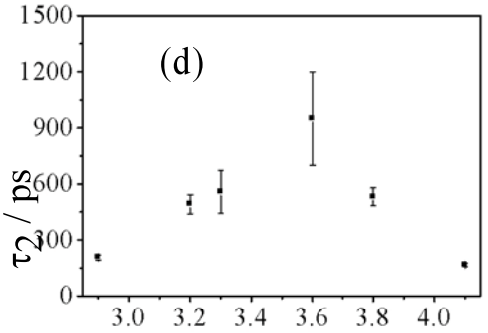

Diameter / nm

Table

W	exciton peak / nm	diameter(calc.) / nm
4	406	2.9
5	418	3.2
6	426	3.4
7	438	3.8
8	446	4.1

d / nm	τ_1 / ps	τ_2 / ps
2.9	11(47%)	207(53%)
3.2	18(45%)	492(55%)
3.3	26(43%)	559(57%)
3.4	38(43%)	long(57%)
3.5	55(37%)	long(63%)
3.6	33(36%)	950(64%)
3.8	28(38%)	532(62%)
4.1	17(39%)	166(61%)